

Quantum Dynamical Approach to Predicting the Optical Pumping Threshold for Lasing in Organic Materials

Bin Zhang[†] and Zhigang Shuai^{*,‡}

[†]*MOE Key Laboratory of Organic OptoElectronics and Molecular Engineering, Department of Chemistry, Tsinghua University, Beijing 100084, China.*

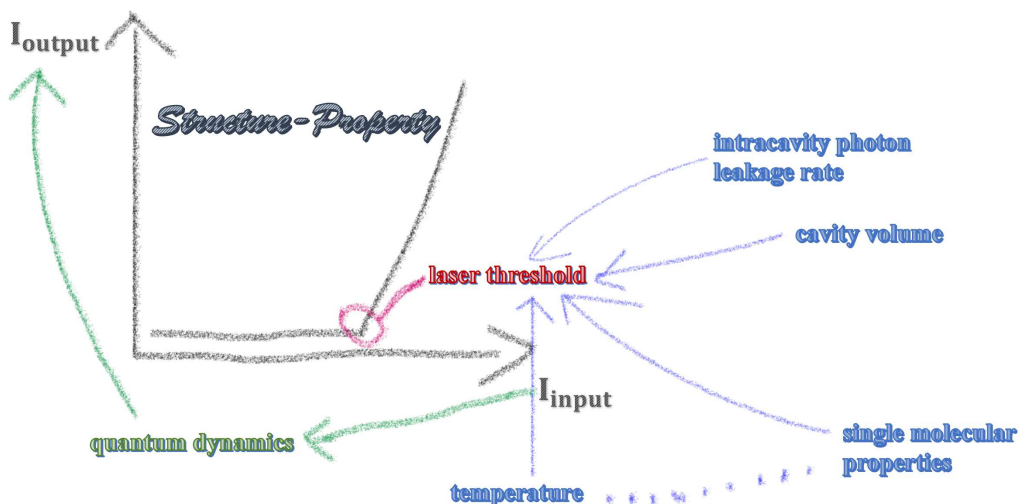
[‡]*School of Science and Engineering, The Chinese University of Hong Kong, Shenzhen, Guangdong 518172, P R China and MOE Key Laboratory of Organic OptoElectronics and Molecular Engineering, Department of Chemistry, Tsinghua University, Beijing 100084, P R China.*

E-mail: shuaizhigang@cuhk.edu.cn

Abstract

We present a quantum dynamic study on organic lasing phenomena, which is a challenging issue in organic optoelectronics. Previously, phenomenological method has achieved success in describing experimental observation. However, it cannot directly bridge the laser threshold with molecular electronic structure parameters and cavity parameters. Quantum dynamics method for describing organic lasing and obtaining laser threshold is highly expected. In this Letter, we first propose a microscopic model suitable for describing the lasing dynamics of organic molecular system and we apply the time-dependent wave-packet diffusion (TDWPD) to reveal the microscopic quantum dynamical process for the optical pumped lasing behavior. Lasing threshold is obtained from the onset of output as a function of optical input pumping. We predict that the lasing threshold has an optimal value as function of the cavity volume

and depends linearly on the intracavity photon leakage rate. The structure-property relationships between molecular electronic structure parameters (including the energy of molecular excited state, the transition dipole and the organization energy) and the laser threshold obtained through numerical calculations are in qualitative agreement the experimental results, which also confirms the reliability of our approach. This work is beneficial to understanding the mechanism of organic laser and optimizing the design of organic laser materials.



TOC Figure

The development of organic solid-state lasers (OSSL) have been greatly promoted over the past few years, due to their wide-range wavelength and low-cost fabrication.^{1,2,6,10,14,15} As we know, organic lasers have been developed for twenty years,²⁴ including the optically pumped laser,^{14,15} the electrically pumped laser^{22,28} and the polariton laser.^{9,26,31} At present, the most mature research of OSSLs are the optically pumped laser. Thanks to the optimization of the gain medium, the high-Q cavity feedback structure and the excellent optical excitation system, the performance of the optically pumped laser has been remarkable improved.²⁴ And, the high-Q optical cavity has become a new way to manipulate the molecular photophysical properties by light-matter coupling. Meanwhile, the theoretical design of organic laser molecules has attracted lots of attention. In the previous work of our group,^{28,34} the computational selection strategies for optically pumped and electrically pumped organic laser molecules have been proposed. Compared to the theoretic-

cal design of laser molecules, there are still few researches on the mechanism of organic lasers, particularly the dynamic process of intracavity photons.

The formation of laser requires an optical gain to compensate the photons leakage in a optical cavity.^{2,14,24} The laser threshold is a crucial parameter to describe organic laser performance. The laser threshold is a particular pump power. When the pump power is larger than the laser threshold, the output power not only increases significantly, but also increases linearly with the input power. Above the laser threshold, the larger output power for a given input power corresponds to the larger slope. It is easy to understand that the lifetime of the exciton and photon in the cavity is very important for the laser threshold. And, increasing the lifetime of exciton and photon can reduce the laser threshold. Excellent laser performance usually corresponds to low laser threshold. Based on phenomenological theory, Adachi's group has been studied the influence of different excitonic losses and photonic leakages on the organic laser threshold of organic lasers under optical and electrical excitations.^{35,36} However, the phenomenological method cannot directly connect between laser threshold and cavity parameters, molecular electronic structure parameters. In this paper, we directly relate the input variable and the output variable of organic lasers to obtain the lasing threshold base on the quantum dynamical method. And then, we investigate the structure-property relationships between laser threshold and cavity parameters (including intracavity photon leakage rate, cavity volume), molecular electronic structure parameters (including the energy of molecular excited state, the transition dipole and the organization energy). Finally, we obtain the physical picture of organic lasers and the related structure-property relationships. The outline of this paper is as follows: First, we extend the TDWPD^{5,7,12,32} method including the light-matter interaction for describing the organic laser in dissipative cavity. Then, combining the extended TDWPD coupled with properly electronic structure calculations of 4,4'-bis[(N-carbazole)styryl]biphenyl (BSBCz)¹⁸ to investigate the structure-property relationship between the intracavity photon leakage rate, cavity volume, single molecular electronic structure properties and the laser threshold. Finally, we investigate the influence of the temperature and the external field duration on the laser threshold. The proposed formalism and the structure-property relationship is beneficial to understanding the

mechanism of organic laser and optimizing the design of organic laser materials.

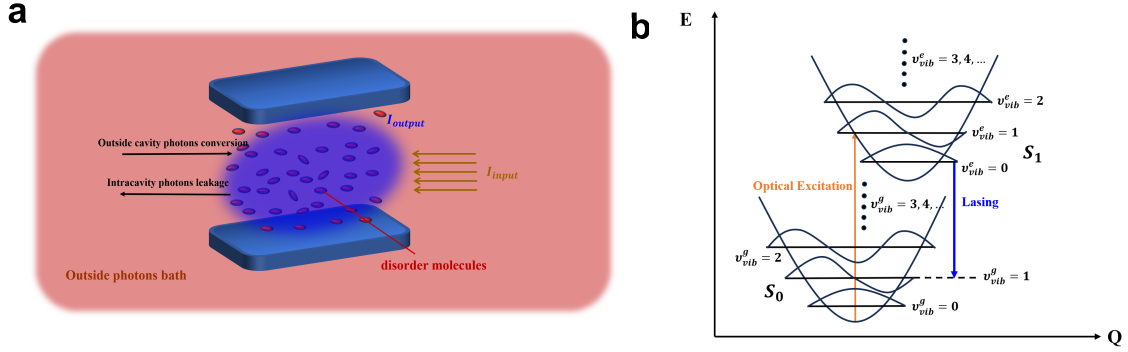


Figure 1: Panel a: Schematic graph of organic lasers in dissipative cavity; Panel b: The molecular four-level energy system, where E is energy, Q is the vibrational coordinate.

In this paper, we study the system which is N identical molecules inside a dissipative optical cavity. The interaction strength between the i th molecule and the intracavity photon $\hbar g_i$ can be written as^{16,29}

$$\hbar g_i = |\vec{\mu}_{eg}| \sqrt{\frac{\hbar \omega_p}{2 \epsilon_0 \epsilon_\infty V}} \cos \theta_i \quad (1)$$

where $\vec{\mu}_{eg}$ is the transition dipole moment (TDM) of the S_1 state; ω_p is the frequency of the intracavity photon; ϵ_0 is the vacuum permittivity; ϵ_∞ is the optical dielectric constant of the matrix inside the cavity; V is the cavity mode volume; and θ_i is the angle between the TDM of the i th S_1 and the intracavity photon. Within the random orientation model, disorder molecules are independent of each other. So, the lasing process of each molecule can be independently studied. And, we assume that each effective molecule only couples one intracavity photon, and they compose a subsystem that is also independent each other. And, the effective molecular number is $N_{eff} = N/\sqrt{3}$. So, we can use the quantum dynamics method to calculate the dynamical properties inside the subsystem including one-molecule and one-photon and then obtain the properties of the total intracavity system. The effective coupling $\hbar \bar{g}$ can be expressed as

$$\hbar \bar{g} = \frac{1}{\sqrt{3}} |\vec{\mu}_{eg}| \sqrt{\frac{\hbar \omega_p}{2 \epsilon_0 \epsilon_\infty V}} \quad (2)$$

In the following text, we use the cavity length L_{cavity} to replace the cavity volume $V = L_{cavity}^3$. And, we use V_{eP} to replace the effective exciton-photon coupling $\hbar\bar{g}$. To describe the organic lasing dynamics in dissipative cavity, the total Hamiltonian can be expressed as

$$\begin{aligned}\hat{H}(t) &= \hat{H}_e(t) + \hat{H}_{photon} + \hat{H}_{phonon} + \hat{H}_{loss} + \hat{H}_{e-photon} + \hat{H}_{e-phonon} + \hat{H}_{photon-loss} \\ &= \hat{H}_E(t) + \hat{H}_{E-bath} + \hat{H}_{bath}\end{aligned}\quad (3)$$

Here, $\hat{H}_e(t)$, \hat{H}_{phonon} , $\hat{H}_{e-phonon}$, \hat{H}_{photon} , $\hat{H}_{e-photon}$, \hat{H}_{loss} and $\hat{H}_{photon-loss}$ denote the Hamiltonian for exciton, the vibrations (or phonon), the exciton-phonon couplings, the intracavity photon, the light-matter interaction, the outside cavity bath and the intracavity photon-outside cavity bath coupling, respectively. And, $\hat{H}_E(t) = \hat{H}_e(t) + \hat{H}_{photon} + \hat{H}_{e-photon}$, $\hat{H}_{E-bath} = \hat{H}_{e-phonon} + \hat{H}_{photon-loss}$ and $\hat{H}_{bath} = \hat{H}_{phonon} + \hat{H}_{loss}$. The Hamiltonian inside the intracavity subsystem including one-molecule and one-photon can be written as

$$\left\{ \begin{aligned}\hat{H}_e(t) &= \varepsilon_g |g\rangle\langle g| + \varepsilon_e |e\rangle\langle e| - \hat{\mu}_{eg} \cdot \vec{E}_{pump}(t) \\ \hat{H}_{photon} &= \hbar\omega_P (\hat{c}_P^\dagger \hat{c}_P + \frac{1}{2}) \\ \hat{H}_{phonon} &= \sum_{j=1}^{N_{ph}^e} \hbar\omega_j^e (\hat{a}_{ej}^\dagger \hat{a}_{ej} + \frac{1}{2}) \\ \hat{H}_{loss} &= \sum_{j=1}^{N_b^P} \hbar\omega_j^P (\hat{b}_{Pj}^\dagger \hat{b}_{Pj} + \frac{1}{2}) \\ \hat{H}_{E-photon} &= V_{eP} |e\rangle\langle g| \hat{c}_P + h.c. \\ \hat{H}_{E-phonon} &= \sum_{j=1}^{N_{ph}^e} C_j^e (\hat{a}_{ej}^\dagger + \hat{a}_{ej}) |e\rangle\langle e| \\ \hat{H}_{photon-loss} &= \sum_{j=1}^{N_b^P} C_j^P (\hat{b}_{Pj}^\dagger + \hat{b}_{Pj}) (\hat{c}_P^\dagger + \hat{c}_P)\end{aligned}\right.\quad (4)$$

And, ε_g , ω_P and ε_e is the energy of ground state $|g\rangle$, the photonic state $\hat{c}_P^\dagger|g\rangle$ and the localized singlet excited state $|e\rangle$, respectively. In this work, the phonon and the outside cavity bath are identified by a collection of harmonic oscillators. C_{ej} is the mode-specific electron-vibrational coupling

strength, and it is determined by the spectral density $J_e(\omega) = \pi \sum_j C_{e_j}^2 \delta(\omega - \omega_j^e)$. C_j^P represents the intracavity photon-outside cavity bath coupling strength, and it is determined by the spectral density $J_P(\omega) = \pi \sum_j C_j^{P2} \delta(\omega - \omega_j^P)$. Here, we set $\vec{\mu}_{eg} \cdot \vec{E}_{pump}(t) \approx |\mu_{eg}| E_{pump}(t) / \sqrt{3}$ which is also the result based on the random orientation approximation. The external field $E_{pump}(t)$ is $E_{pump}(t) = \frac{E_0}{\sqrt{2\pi\sigma}} e^{-\frac{t^2}{2\sigma^2}} \cos(\omega_{pump}t)$. And, σ , E_0 and ω_{pump} are the field duration, the field strength and the field frequency, respectively. In the following text, we use μ_{eg} to replace $|\mu_{eg}|$. For resonance excitation, we set $\hbar\omega_{pump} = \varepsilon_e$. The formulas and the parameters setting of their spectral density will be described in detail in the following text. In the quantum dynamic simulations, we adopt TDWPD^{5,7,12} because it can be easily applied to large complex systems and extended to incorporate the strong light-matter coupling. Recently, TDWPD method has been extended to include the light-matter interaction and successfully investigated the effect of the optical microcavity on the singlet fission dynamics in organic systems.³² Previous research results have shown that the TDWPD method is indeed suitable for studying the dynamic properties of complex molecular systems incorporating light-matter interaction. The TDWPD method is one of stochastic Schrödinger equations(SSE) where the molecular vibrational motions are described by random fluctuations on each electronic state. And, the dynamical equation can be written as

$$i \frac{\partial}{\partial t} |\Psi(t)\rangle = (\hat{H}_E(t) + \hat{F}(t) - i\hat{L} \int_0^t d\tau \alpha_{T=0}(\tau) e^{i\int_0^\tau \hat{H}_E(\tau') d\tau'} \hat{L}^\dagger e^{-i\int_0^\tau \hat{H}_E(\tau') d\tau'}) |\Psi(t)\rangle \quad (5)$$

where $\hat{H}_E(t)$ is the intracavity system Hamiltonian, $\hat{F}(t)$ is the the stochastic force operator $\hat{F}(t) = \sum_{n,m} F_{nm}(t) |n\rangle \langle m|$, $\alpha_{T=0}(t)$ is the zero-temperature correlation function $\alpha_{T=0}(t) = \sum_j C_j^{n2} e^{-i\omega_j^n t}$, \hat{L} is the projection operator. The states $|n(m)\rangle$ include the ground state $|g\rangle$, the excited state $|e\rangle$ and the intracavity photon state $|P\rangle$. And, $\hat{L} = |e\rangle \langle e|$, $|g\rangle \langle P|$ and $|P\rangle \langle g|$ are correspond to the excited state $|e\rangle$, the ground state $|g\rangle$ and the intracavity photon state $|P\rangle$, respectively. The completely relation is

$$1 = |e\rangle \langle e| + |g\rangle \langle g| + |P\rangle \langle P| \quad (6)$$

In numerical calculations, the wavefunction $|\Psi(t)\rangle$ is written as

$$|\Psi(t)\rangle = A_e(t)|e\rangle + A_g(t)|g\rangle + A_P(t)|P\rangle \quad (7)$$

The differential equations of the time-dependent coefficients $\{A_j(t)\}$ (j=g, e or P) are

$$\left\{ \begin{array}{l} i\frac{\partial}{\partial t}A_e(t) = (\varepsilon_e + F_e(t))A_e(t) + V_{eP}A_P(t) - (\vec{\mu}_{eg} \cdot \vec{E}_{pump}(t))A_g(t) \\ \quad - i\sum_k \int_0^t d\tau \alpha_e(\tau) \langle e|e^{i\int_0^\tau \hat{H}_E(\tau')d\tau'}|e\rangle \langle e|e^{-i\int_0^\tau \hat{H}_E(\tau')d\tau'}|k\rangle A_k(t), \\ i\frac{\partial}{\partial t}A_g(t) = \varepsilon_g A_g(t) + F_g(t)A_P(t) - (\vec{\mu}_{eg} \cdot \vec{E}_{pump}(t))A_e(t) \\ \quad - i\sum_k \int_0^t d\tau \alpha_g(\tau) \langle P|e^{i\int_0^\tau \hat{H}_E(\tau')d\tau'}|P\rangle \langle g|e^{-i\int_0^\tau \hat{H}_E(\tau')d\tau'}|k\rangle A_k(t), \\ i\frac{\partial}{\partial t}A_P(t) = \hbar\omega_P A_P(t) + V_{eP}A_e(t) + F_P(t)A_g(t) \\ \quad - i\sum_k \int_0^t d\tau \alpha_P(\tau) \langle g|e^{i\int_0^\tau \hat{H}_E(\tau')d\tau'}|g\rangle \langle P|e^{-i\int_0^\tau \hat{H}_E(\tau')d\tau'}|k\rangle A_k(t). \end{array} \right. \quad (8)$$

Here, $F_{e(P)}(t)$ is the stochastic force, which can be generated by

$$F_{e(P)}(t) = \sum_k \sqrt{\frac{J_{e(P)}(\omega_k)\Delta\omega}{\pi}} [\sqrt{A(\omega_k)} \cos(\omega_k t + \phi_k) + i\sqrt{B(\omega_k)} \sin(\omega_k t + \phi_k)] \quad (9)$$

with $A(\omega_k) = \coth(\omega_k/2k_B T) + csch(\omega_k/2k_B T)$ and $B(\omega_k) = \coth(\omega_k/2k_B T) - csch(\omega_k/2k_B T)$. $\{\phi_k\}$ is a series of random variables that are uniformly distributed in $[0, 2\pi]$. $\alpha_e(t) = \sum_j C_j^{e2} e^{-i\omega_j^e t}$, $\alpha_P(t) = \sum_j C_j^{P2} e^{-i\omega_j^P t}$ are the zero-temperature correlation function of the exciton-phonon couplings and the intracavity photon-outside cavity bath couplings. From the TDWPD equation Eq. 8, we can obtain the time-dependent coefficients $\{A_j(t)\}$ (j=g, e or P). The population dynamics can be obtained by the stochastic average of $A_{e(g, or P)}(t)$. For instance, the time evolution of population on the i ($i = e, g$ or P)-th state is calculated by $P_i(t) = \langle A_i^*(t)A_i(t) \rangle$. The input variable is the intensity of incident laser pulse is I_{input} , and it can be defined as

$$I_{input} \propto |E_0|^2 \quad (10)$$

where 1.0 a.u. field strength $|E_0|$ corresponds to 3.5094×10^{13} KW/cm² input intensity I_{input} .^{4,27} Although I_{input} is the input variable, we directly change the field strength E_0 in numerical calculations. The output variable is I_{output} , which is the steady-state photon density inside the cavity, and it can be defined as

$$I_{output} = \lim_{t \rightarrow \infty} P_P(t) c_M N_A / \sqrt{3} \quad (11)$$

where $P_P(t)$ is the population of photon state inside the intracavity subsystem including one-molecule and one-photon, $c_M = N/V$ is the doping concentration of the molecule, N_A is the Avogadro constant. $\lim_{t \rightarrow \infty} P_P(t)$ is the population of the intracavity photon state when the intracavity system reaches the thermal equilibrium state. It is noteworthy that we should use the effective molecular number $N_{eff} = N/\sqrt{3}$ to calculate the output variable I_{output} due to the random orientation approximation.²⁹ For the intracavity system including exciton, phonon, and photon, we use different intensities of external fields I_{input} to excite molecules and transfer the population to the intracavity photon state through exciton-intracavity photon coupling. When the steady-state state is reached, the intracavity photon density is calculated to obtain the output variable I_{output} .

The Molecular Properties of BSBCz. In this paper, we use BSBCz as a test molecule. In the previous work of our group, BSBCz not only has excellent the photo-pumped laser performance, but also has excellent the electro-pumped laser performance.²⁸ We use TD-B3LYP/6-31g* to calculate the single molecule properties of BSBCz by Gaussian16.¹⁷ Theoretically predicted that the energy of S_1 state is 2.472 eV, and the transition dipole is 6.839 a.u.. Based on the knowledge of electronic structure, we compute the rate constants of different physical processes by the TVCF rate formalism.^{11,23,30} All rate constant calculations and are performed via thermal vibration correlation function (TVCF) method in MOMAP 2021A.^{3,21,25} Theoretically predicted that the radiative rate of S_1 state k_r is 6.5×10^8 s⁻¹ as well as the internal conversion rate of S_1 state k_{ic} is 1.5×10^8 s⁻¹, which are consistent with the numerical results in Ref. 28. The Lorentzian

broadening $FWHM = 200 \text{ cm}^{-1}$ has been used to k_{ic} for converge. Here, we also display the molecular reorganization energy distribution, shown in Figure 2. In the following text, we get the intramolecular vibration spectral density based on the reorganization energy distribution. Our approach cannot does not destroy the molecular four-level energy system (see Figure 1 b) due to including all of vibration information.

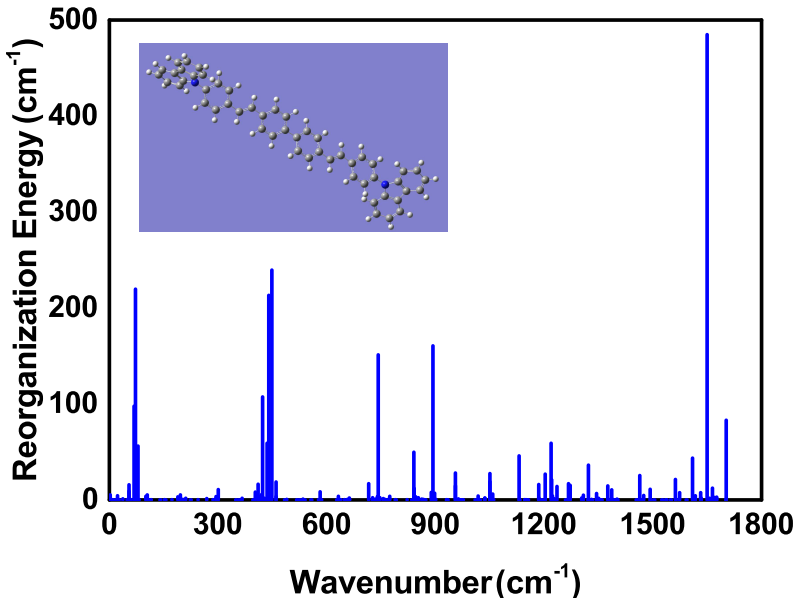


Figure 2: The reorganization energy distribution of BSBCz. The inset shows the chemical structure of BSBCz.

The Quantum Dynamics Results of Organic Lasers. Next, we calculate the laser dynamics, as well as the structure-property relationship between the intracavity photon-outside cavity bath coupling strength, cavity size, single molecular electronic structure properties and the laser threshold. Before the numerical calculations, we summarize the extended TDWPD method and the calculation method of the main physical quantities involved in this Letter. In this paper, we study the system which is N identical molecules inside an dissipative optical cavity. Based on the random orientation approximation, the disorder molecules inside the cavity are independent of each other. The lasing process of each molecule can be independently studied. And, we assume that each effective molecule only couples one intracavity photon, and they compose a subsystem that is also

independent each other. So, we can use the quantum dynamics method to calculate the dynamical properties inside the subsystem including one-molecule and one-photon and then obtain the properties of the total intracavity system. And, the effective molecular number is $N_{eff} = N/\sqrt{3}$. In the quantum dynamic simulations, we adopt TDWPD^{5,7,12} because it can be easily applied to large systems and extended to incorporate the strong light-matter coupling. Recently, TDWPD method has been extended to include the light-matter interaction and successfully investigated the effect of the optical microcavity on the singlet fission dynamics in organic system.³² Previous research results have shown that the TDWPD method is indeed suitable for studying the dynamic properties of complex molecular systems incorporating light-matter interaction. The TDWPD method is one of stochastic Schrödinger equations(SSE) where the molecular vibrational motions are described by random fluctuations on each electronic state. From the TDWPD equation Eq. 8, we can obtain the time-dependent coefficients $\{A_j(t)\}$ ($j=g, e$ or P). The population dynamics is thus obtained by the stochastic average of $A_{e(g, or P)}(t)$. For example, the time evolution of population on the i ($i = e, g$ or P)-th state is calculated by $P_i(t) = \langle A_i^*(t)A_i(t) \rangle$. The input variable is I_{input} ($I_{input} \propto |E_0|^2$, see Eq. 10) is the input variable is the intensity of incident laser pulse $E_{pump}(t)$, and we change the intensity of incident laser pulse by changing the value of the field strength E_0 in the numerical calculations. The output variable I_{output} ($I_{output} = \lim_{t \rightarrow \infty} P_P(t)c_M N_A/\sqrt{3}$, see Eq. 11) is the steady-state photon density inside the cavity. And, the doping concentration c_M is 0.15×10^{-3} M.¹⁸ Next, we can obtain the laser threshold I_{thred} and the field strength threshold E_{thred} through the inflection point of the I_{output} - I_{input} curve. Following the preceding calculation process, we can obtain the structure-property relationships between laser threshold I_{thred} and cavity parameters, molecular electronic structure parameters.

For our microscopic model, the coupling between the intracavity photons and bath is actually the coupling between the intracavity photons and the continuous photon environment outside the cavity. It leads to the intracavity photons leak into the photon environment outside the cavity, manifested as the quenching of the intracavity photons. Similarly, if there are no intracavity photons, and the intracavity photons-bath coupling is relatively large, the photons outside the cavity

will also penetrate into the cavity (at the initial time, the initial state of the photon environment is thermal equilibrium distribution). So, there will be a small amount of population of the intracavity photon state without external field $E_{pump}(t)$ excitation. The schematic graph is shown as Figure 1. The population dynamics of the intracavity system at exciton-photon coupling V_{eP} also confirms the physical picture, shown in Figure S5, S6 (see the Supporting Information). For exciton-phonon coupling C_{ej} , is described by the spectral density with broadened stick-spectra of pseudo-local phonon modes,^{8,19} $J_e(\omega) = \frac{1}{\pi} \sum_k \frac{\lambda_k \omega \gamma}{(\omega - \omega_k)^2 + \gamma^2}$ which includes the information of all vibrational modes to study the dynamical properties of the realistic molecular system with a uniform broadening factor of $\gamma = 40.0$ meV to smoothly generate fluctuation energies.²⁰ The reorganization energy λ_k is calculated via the vibrational modes of the monomer, shown in Figure 2. The coupling strength C_j^P between intracavity photon and we use the Debye spectral density $J_P(\omega) = \frac{2\lambda_P \omega \omega_P^c}{\omega^2 + \omega_P^c{}^2}$ to describe bath, which is consistent with David Reichman's recent work.³⁷ And, we set the characteristic frequency of the photon environment outside the cavity ω_P^c is $\omega_P^c = 1450$ cm⁻¹. According to the spectral density $J_P(\omega)$, we can calculate the corresponding leakage rate of the intracavity photon $\Gamma_P = \frac{1}{\tau_P} = \frac{2J_P(\omega_P)}{1 - e^{-\beta\omega_P}}$ where τ_c is the intracavity photon lifetime and $\beta = \frac{1}{k_B T}$ with the Boltzmann constant k_B and temperature $T(T = 300$ K), and then obtain the quality of cavity(Q value) $Q = \frac{1}{2} \frac{\omega_P}{\Gamma_P}$.^{35,36} The relevant results are shown in the Table 1. The exciton-photon coupling strength is shown in the Table 3. In this paper, we set the resonance between the external field energy and the S_1 state of molecule. From the Figure 7, we can see that the duration σ is almost independent of the laser threshold. Without loss of generality, we set the σ to be 30.0 fs later.

Table 1: The intracavity photon leakage rate Γ_P and the quality of cavity Q to different intracavity photon-outside cavity bath coupling strength λ_P .

$\lambda_P(meV)$	0.0	0.5	1.0	5.0	10.0	20.0	50.0	100.0	200.0
$\Gamma_P(meV)$	0.0	0.1447	0.289	1.447	2.894	5.787	14.47	28.94	57.87
Q	infinity	8542.64	4271.32	854.26	427.13	213.57	85.43	42.71	21.36

Firstly, we calculated the structure-property relationship between the intracavity photon-outside cavity bath coupling strength λ_P , cavity length L_{cavity} , and laser threshold I_{thred} . The calculated re-

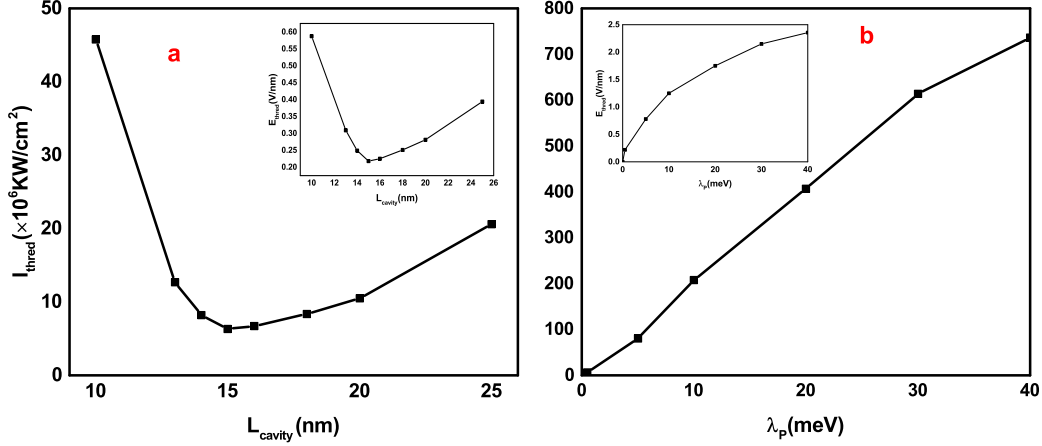


Figure 3: The structure-property relationship between cavity length L_{cavity} (Panel a), the intracavity photon-outside cavity bath coupling strength λ_P (Panel b), and laser threshold I_{thred} . The inset shows the structure-property relationship about the field strength threshold E_{thred} .

Table 2: The intracavity photon leakage rate Γ_P and the quality of cavity Q to different intracavity photon frequency ω_P .

$\omega_P(eV)$	2.0	2.2	2.4	2.6	2.8	3.0
$\Gamma_P(meV)$	0.1783	0.1624	0.1490	0.1376	0.1279	0.1190
Q	5607.37	6775.48	8054.84	9445.44	10947.30	12560.40

sults are shown in the Figure 3. Figure 3a shows the structure-property relationship between the intracavity photon-outside cavity bath coupling strength λ_P , cavity length L_{cavity} , and laser threshold I_{thred} , while Figure 3b shows the population dynamics of photon state. Without loss of generality, we set that the quality of this order of magnitude is often used for research in experiments, the λ_P is 0.5 meV. From the calculation results, it can be seen that the laser threshold increases with L_{cavity} . The laser intensity threshold first decreases and then increases, which can be understood from physical picture. The external field will destroy the equilibrium state of the system and bring it to a new stable state. Only when the intensity of the external field $E_{pump}(t)$ is sufficient to break the equilibrium state of the system, lasing phenomenon will happened, which manifest as the broken line of $I_{output}-I_{input}$ curve and as a sudden change on the dynamics of intracavity photon state. When the coupling strength between exciton and intracavity photon is large enough, a stronger external field is required to disrupt the equilibrium state of the intracavity system; And,

Table 3: The exciton-photon coupling V_{ep} to different cavity length L_{cavity} .

$L_{cavity}(nm)$	10.0	13.0	15.0	16.0	18.0	20.0	25.0
$V_{ep}(meV)$	31.55	21.08	17.18	15.44	12.94	11.16	7.91

when L_{cavity} is very large, the population transfer between exciton and intracavity photon is suppressed due to the small coupling strength between exciton and the intracavity photon. Therefore, a stronger external field is needed to produce a sudden change on the dynamics of intracavity photon state. From this physical picture, it is not difficult to understand that the laser threshold varies with L_{cavity} . It is worth noting that there is no direct correspondence between the laser threshold and the steady-state population of the intracavity photon state. This is because the laser threshold is controlled by the short-time excitation of the external field, and it belongs to the short-time dynamical property; the steady-state population of the intracavity photon state is controlled by the interaction of different components in total system, which belongs to the long-time dynamical property. So, the phenomenon of the low laser threshold and the large steady-state population of the intracavity photon state may happen. This is indeed reflected in Figure 4. The population dynamics of ground state, local excited state and photon state at different cavity length are shown in Figure S1, S2 and S3 (see the Supporting Information). Of course, when the cavity length L_{cavity} is very large (the exciton-photon coupling V_{ep} is smaller than the intracavity photon leakage rate Γ_P), the steady-state population of the intracavity photon state will indeed show a monotonic decreasing trend as L_{cavity} increases, shown in Figure S4 (see the Supporting Information). From Figure 3b, we can see that the laser intensity threshold has a linear relationship as the intracavity photon-bath coupling strength increasing. And, the laser intensity threshold is inversely proportional to the quality of cavity. When the intracavity photon-bath coupling strength is set to 0.0, the laser intensity threshold is also equal to zero. The results are shown in Figure S7 (see the Supporting Information). This indicates that when we change the the intracavity photon-bath coupling strength values, we can obtain laser thresholds of any size. Base on this linear relationship, we are not limited to the specific values of the laser threshold, but focus on the structure-property relationship. It is worth

noting that as the intracavity photon leakage rate increases, it does lead to an increase in the initial population of the intracavity photon state and a decrease in the steady-state population of the intracavity photon state, shown in Figure 5.

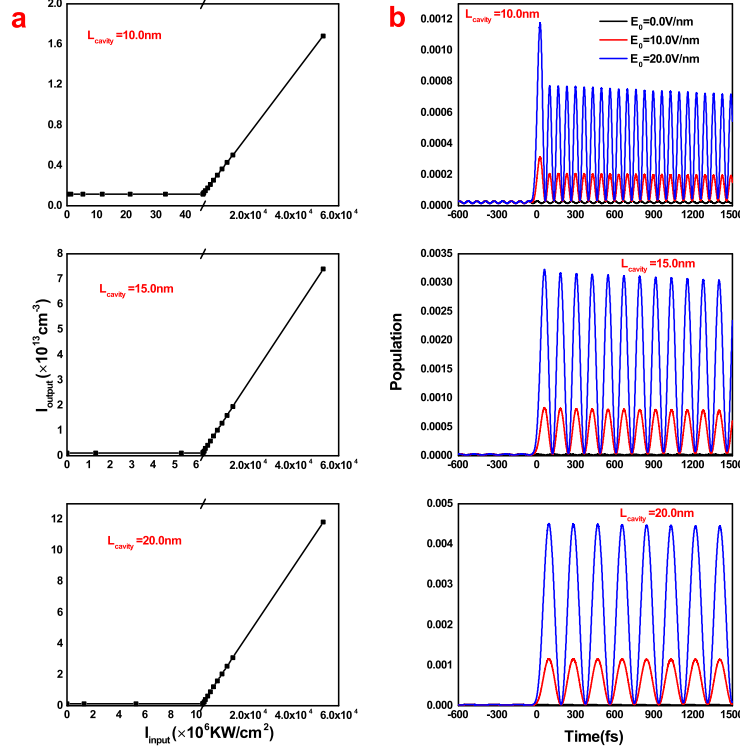


Figure 4: Panel a: The $I_{output}-I_{input}$ curve at different cavity length L_{cavity} ; Panel b: The population dynamics of photon state inside the subsystem including one-molecule and one-photon at different cavity length L_{cavity} .

Next, we calculate the structure-property relationship between the electronic structure properties of single molecule and the laser threshold. We investigate the influence of the energy of S_1 state ϵ_e , the molecular transition dipole μ_{eg} and the reorganization energy λ_m on the laser threshold I_{thred} . Here, we set $L_{cavity} = 15.0 \text{ nm}$, $\lambda_p = 0.5 \text{ meV}$. For the calculation of reorganization energy, we use Debye spectral density $J(\omega) = \frac{2\lambda_m\omega\omega_c}{\omega^2 + \omega_c^2}$ to describe the exciton-phonon coupling. Here, we change the reorganization energy λ_m . And, the characteristic frequency ω_c is set to 1450.0 cm^{-1} .^{8,19,32} The calculated results are shown in the Figure 6. From the results, we can see that the laser threshold I_{thred} are monotonically decreasing as the molecular S_1 state energy ϵ_e and the molecular transition dipole μ_{eg} increasing. But, the reorganization energy λ_m cannot

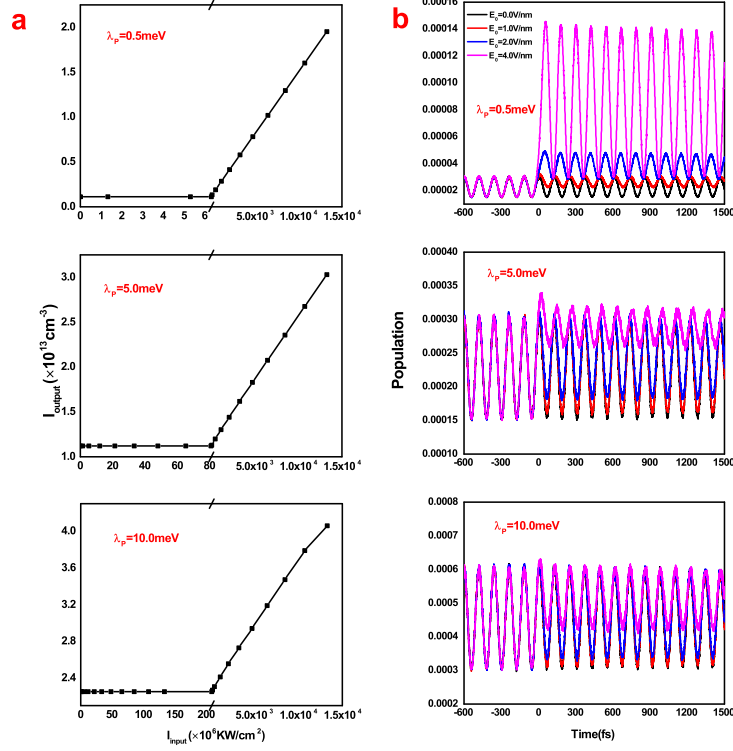


Figure 5: Panel a: The I_{output} - I_{input} curve at different intracavity photon-outside cavity bath coupling strength λ_p ; Panel b: The population dynamics of photon state inside the subsystem including one-molecule and one-photon at different intracavity photon-outside cavity bath coupling strength λ_p .

change the laser threshold I_{thred} . The molecular S_1 state energy ϵ_e and the molecular transition dipole μ_{eg} are inversely proportional to the laser threshold I_{thred} . This is consistent with the experimental results.³³ When the molecular S_1 state energy ϵ_e decreases, the intracavity photons will be quenched faster (shown in Table 2), which leads to the increase of the laser threshold I_{thred} . The decreasing of the molecular transition dipole μ_{eg} will weaken the ability of external fields to disrupt the initial steady-state of the intracavity system, leading to the increase of the laser threshold I_{thred} . Although the reorganization energy λ_m has almost no effect on the laser threshold I_{thred} . However, the increasing of the reorganization energy λ_m can reduce the steady-state population of intracavity photon state, which does hinder light amplification in the cavity. The calculated population dynamics of intracavity photon state is shown in Figure S8 (see the Supporting Information). As we know, Debye spectral density is very suitable for describing the low-frequency vibrational modes of molecule. When we increase λ_m , the low frequency vibration modes are enhanced, and

the high-frequency modes are almost unaffected. Therefore, the molecular "four-level" energy system is ruined. This is consistent with the conclusion proposed by Ref. 13. In this work, we cannot consider the influence of the molecular aggregation effect on the laser threshold I_{thred} . And, we will extend the current work to investigate the influence of the molecular aggregation effect on the laser threshold I_{thred} in our future work.

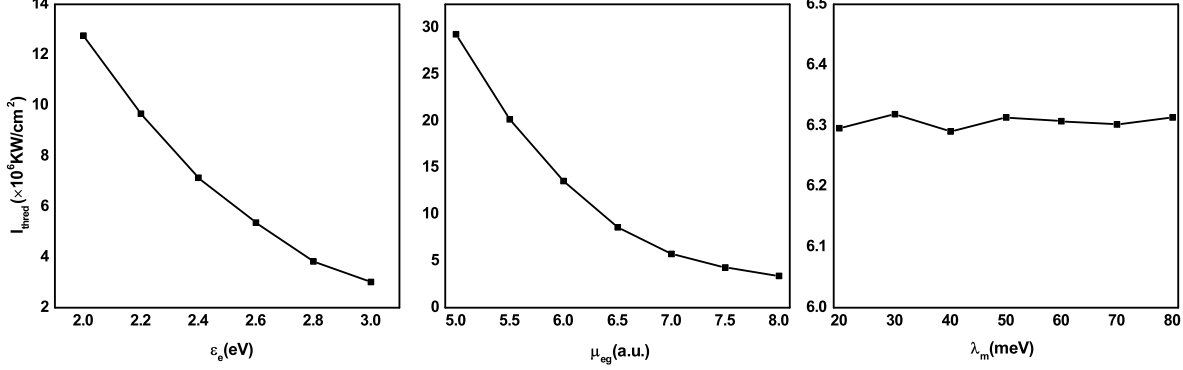


Figure 6: The structure-property relationship between the molecular S_1 state energy ϵ_e , the molecular transition dipole μ_{eg} and the reorganization energy λ_m and the laser threshold I_{thred} .

Finally, we investigate the effects of temperature T and external field duration σ on the laser threshold I_{thred} , and the calculated results are shown in the figure 7. From the calculation results, we can see that temperature T and external field duration σ cannot change the laser threshold I_{thred} . From the population dynamics of intracavity photon state, it can be seen that the increasing of temperature T can accelerate the relaxation of the intracavity system. And, the increasing of the external field duration σ can decrease the external field strength at $t = 0.0$, thereby reducing the population of intracavity photon state. Although the action time of the external field $E_{pump}(t)$ will increase as the duration σ increasing, a smaller duration σ is indeed beneficial for increasing the steady-state population of intracavity photon state. It is worth noting that increasing duration σ does not mean that the external field $E_{pump}(t)$ can exhibits the performance of continuous wave. when the duration σ approaches infinity, the external field $E_{pump}(t)$ has no effect on the intracavity system.

To conclude, based on the Time-dependent wavepacket diffusion (TDWPD) method in coupled with light-matter interaction, we develop a microscopic quantum dynamic approach to describe

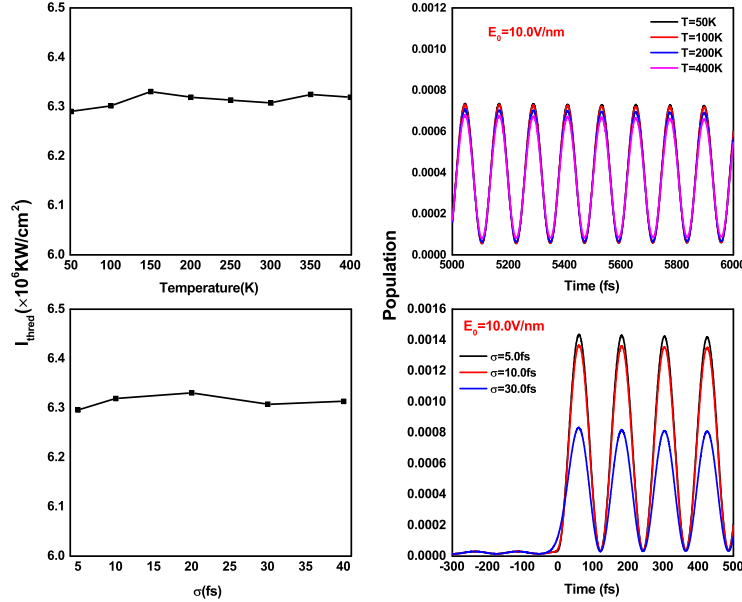


Figure 7: Panel left: The relationship between temperature T , duration σ and the laser threshold I_{thred} ; Panel right: The population dynamics of photon state inside the subsystem including one-molecule and one-photon at different temperature T and duration σ .

the organic lasing phenomena in dissipative cavity. The extended TDWPD is applied to investigate the structure-property relationships between the lasing threshold and the intracavity photon-outside cavity bath coupling strength, cavity size, single molecular electronic structure properties. The following conclusions are drawn: (i) A microscopic model suitable for describing the lasing dynamics of organic molecular system has been constructed, which can be used to describe the structure-property relationships between laser threshold and cavity parameters, molecular electronic structure parameters; (ii) The microscopic physical picture of organic laser is proposed. The photons outside the cavity can penetrate into the cavity, leading to the thermal equilibrium state in the cavity. Only when the intensity of the external field is sufficient to break the equilibrium state of the intracavity system, lasing phenomenon will happened; (iii) The laser threshold decreases first and then increases as the cavity size increases, and there is an optimal value that can be understood from physical picture. The laser threshold increases linearly with increasing the intracavity photon-outside cavity bath coupling strength, exhibiting the monotone decreasing tendency with the increase of the cavity quality value (Q value), which is consistent with the experimental results; (iv) The reorganization energy cannot change the laser threshold. The larger the reorganization en-

ergy leads to the reduction of the steady-state population of intracavity photon state. The energy of S_1 state and the transition dipole are inversely proportional to the laser threshold, which is consistent with the experimental conclusion. The proposed formalism and structure-property relationship is beneficial to understanding the mechanism of organic laser and optimizing the design of organic laser materials.

ACKNOWLEDGEMENT

Financial supports from Shenzhen Science and Technology Program and the National Natural Science Foundation of China (Grant Nos. 21788102) as well as the Ministry of Science and Technology of China through the National Key R&D Plan (Grant No. 2017YFA0204501) are gratefully acknowledged.

Supporting Information Available

The supplementary materials include the population dynamics of ground state, local excited state and photon state inside the subsystem including one-molecule and one-photon at different cavity length, The I_{output} - I_{input} curve at cavity length $L_{cavity} = 15.0$ nm and the intracavity photon-outside cavity bath coupling strength $\lambda_P = 0.0$ meV, the population dynamics of photon state inside the subsystem including one-molecule and one-photon at different reorganization energy λ_m .

References

- (1) Fichou, D.; Delysse, S.; Nunzi, J. M. First evidence of stimulated emission from a monolithic organic single crystal: α -Octithiophene. *Adv. Mater.* **1997**, *9*, 1178–1181.
- (2) Samuel, I. D. W.; Turnbull, G. A. Organic semiconductor lasers. *Chem. Rev.* **2007**, *107*, 1272–1295.

- (3) Peng, Q.; Yi, Y.; Shuai, Z.; Shao, J. Toward Quantitative Prediction of Molecular Fluorescence Quantum Efficiency: Role of Duschinsky Rotation. *J. Am. Chem. Soc.* **2007**, *129*, 9333–9339.
- (4) Sun, J.; Guo, Z. Y.; Liang, W. Z. Harmonic generation of open-ended and capped carbon nanotubes investigated by time-dependent Hartree-Fock theory. *Phys. Rev. B* **2007**, *75*, 195438.
- (5) Zhong, X. X.; Zhao, Y. Charge Carrier Dynamics in Phonon-Induced Fluctuation Systems from Time-Dependent Wavepacket Diffusion Approach. *J. Chem. Phys.* **2011**, *135*, 134110.
- (6) Chénais, S.; Forget, S. Recent advances in solid-state organic lasers. *Polym. Int.* **2012**, *61*, 390–406.
- (7) Zhong, X. X.; Zhao, Y. Non-Markovian Stochastic Schrödinger Equation at Finite Temperatures for Charge Carrier Dynamics in Organic Crystals. *J. Chem. Phys.* **2013**, *138*, 014111.
- (8) Berkelbach, T. C.; Hybertsen, M. S.; Reichman, D. R. Microscopic Theory of Singlet Exciton Fission. II. Application to Pentacene Dimers and the Role of Superexchange. *J. Chem. Phys.* **2013**, *138*, 114103.
- (9) Schneider, C.; Rahimi-Iman, A.; Kim, N. Y.; Fischer, J.; Savenko, I. G.; Amthor, M.; Lerner, M.; Wolf, A.; Worschech, L.; Kulakovskii, V. D.; Shelykh, I. A.; Kamp, M.; Reitzenstein, S.; Forchel, A.; Yamamoto, Y.; Höfling, S. An electrically pumped polariton laser. *Nature* **2013**, *497*, 348–352.
- (10) Cui, Q. H.; Zhao, Y. S.; Yao, J. Controlled synthesis of organic nanophotonic materials with specific structures and compositions. *Adv. Mater.* **2014**, *26*, 6852–6870.
- (11) Shuai, Z.; Peng, Q. Excited States Structure and Processes: Understanding Organic Light-Emitting Diodes at the Molecular Level. *Phys. Rep.* **2014**, *537*, 123–156.
- (12) Lu, H.; Ke, Y. L.; Zhong, X. X.; Zhao, Y. Time-Dependent Wavepacket Diffusion Method and Its Applications in Organic Semiconductors. *Int. J. Quantum Chem.* **2015**, *115*, 578–588.

- (13) Ma, L.; Wu, Z.; Zhou, G.; Yuan, F.; Yu, Y.; Yao, C.; Ning, S.; Hou, X.; Li, Y.; Wang, S.; Gong, Q. The Molecular Picture of Amplified Spontaneous Emission of Star-Shaped Functionalized-Truxene Derivatives. *J. Mater. Chem. C* **2015**, *3*, 7004–7013.
- (14) Kuehne, A. J. C.; Gather, M. C. Organic lasers: recent developments on materials, device geometries, and fabrication techniques. *Chem. Rev.* **2016**, *116*, 12823–12864.
- (15) Gierschner, J.; Varghese, S.; Park, S. Y. Organic single crystal lasers: a materials view. *Adv. Opt. Mater.* **2016**, *4*, 348–364.
- (16) Ebbesen, T. W. Hybrid Light-Matter States in a Molecular and Material Science Perspective. *Acc. Chem. Res.* **2016**, *49*, 2403–2412.
- (17) Frisch, M. J.; Trucks, G. W.; Schlegel, H. B.; Scuseria, G. E.; Robb, M. A.; Cheeseman, J. R.; Scalmani, G.; Barone, V.; Petersson, G. A.; Nakatsuji, H.; et al., Gaussian 16 Revision B.01. 2016; Gaussian Inc. Wallingford CT.
- (18) Sandanayaka, A. S. D.; Yoshida, K.; Inoue, M.; Qin, C. J.; Goushi, K.; Ribierre, J. C., Matsushima, T.; Adachi, C. Quasi-Continuous-Wave Organic Thin-Film Distributed Feedback Laser. *Adv. Opt. Mater.* **2016**, *4*, 834–839.
- (19) Zang, H.; Zhao, Y.; Liang, W. Z. Quantum Interference in Singlet Fission: J- and H-Aggregate Behavior. *J. Phys. Chem. Lett.* **2017**, *8*, 5105–5112.
- (20) Zhu, Z. Y., Zang, H.; Zhao, Y.; Liang, W. Z. Charge Carrier Mobilities and Singlet Fission Dynamics in Thienoquinoidal Compounds. *J. Phys. Chem. C* **2017**, *121*, 22587–22596.
- (21) Shuai, Z.; Peng, Q. Organic Light-Emitting Diodes: Theoretical Understanding of Highly Efficient Materials and Development of Computational Methodology. *Nat. Sci. Rev.* **2017**, *4*, 224–239.
- (22) Sandanayaka, A. S. D.; Matsushima, T.; Bencheikh, F.; Terakawa, S.; Potscavage, Jr. W. J.;

- Qin, C. J.; Fujihara, T.; Goushi, K.; Ribierre, J. C.; Adachi, C. Indication of current-injection lasing from an organic semiconductor. *Appl. Phys. Express* **2019**, *12*, 061010.
- (23) Wang, Y.; Peng, Q.; Ou, Q.; Lin, S.; Shuai, Z. A Novel Molecular Descriptor for Highly Efficient ($\Phi_{TADF} > 90\%$) Transition Metal TADF Au(iii) Complexes. *J. Mater. Chem. A* **2020**, *8*, 18721–18725.
- (24) Jiang, Y.; Liu, Y. Y.; Liu, X.; Lin, H.; Gao, K.; Lai, W. Y.; Huang, W. Organic solid-state lasers: a materials view and future development. *Chem. Soc. Rev.* **2020**, *49*, 5885–5944.
- (25) Shuai, Z. Thermal Vibration Correlation Function Formalism for Molecular Excited State Decay Rates. *Chin. J. Chem.* **2020**, *38*, 1223–1232.
- (26) Ren, J. H.; Liao, Q.; Huang, H.; Li, Y.; Gao, T. G.; Ma, X. K.; Schumacher, S.; Yao, J. N.; Bai, S. M.; Fu, H. B. Efficient Bosonic Condensation of Exciton Polaritons in an H-Aggregate Organic Single-Crystal Microcavity. *Nano Lett.* **2020**, *20*, 7550–7557.
- (27) Sun, J.; Ding, Z. L.; Yu, Y. Q.; Liang, W. Z. Plasmon-enhanced high order harmonic generation of open-ended finite-sized carbon nanotubes: The effects of incident field's intensity and frequency and the interference between the incident and scattered fields. *J. Chem. Phys.* **2020**, *152*, 224708.
- (28) Ou, Q.; Peng, Q.; Shuai, Z. Computational screen-out strategy for electrically pumped organic laser materials. *Nat. Commun.* **2020**, *11*, 4485.
- (29) Ou, Q.; Shao, Y.; Shuai, Z. Enhanced Reverse Intersystem Crossing Promoted by Triplet Exciton-Photon Coupling. *J. Am. Chem. Soc.* **2021**, *143*, 17786–17792.
- (30) Lin, S.; Ou, Q.; Wang, Y.; Peng, Q.; Shuai, Z. Aggregation-Enhanced Thermally Activated Delayed Fluorescence Efficiency for Two-Coordinate Carbene-Metal-Amide Complexes: A QM/MM Study. *J. Phys. Chem. Lett.* **2021**, *12*, 2944–2953.

- (31) Jiang, Z. J.; Ren, A.; Yan, Y. L.; Yao, J. N.; Zhao, Y. S. Exciton-Polaritons and Their Bose-Einstein Condensates in Organic Semiconductor Microcavities. *Adv. Mater.* **2021**, *34*, 2106095.
- (32) Zhang, B.; Zhao, Y.; Liang, W. Z. Joint Effects of Exciton-Exciton and Exciton-Photon Couplings on the Singlet Fission Dynamics in Organic Aggregates. *J. Phys. Chem. C* **2021**, *125*, 1654–1664.
- (33) Oyama, Y.; Mamada, M.; Kondo, A.; Adachi, C. Advantages of naphthalene as a building block for organic solid state laser dyes: smaller energy gaps and enhanced stability. *J. Mater. Chem. C* **2021**, *9*, 4112.
- (34) Lin, S. Y.; Ou, Q.; Shuai, Z. Computational Selection of Thermally Activated Delayed Fluorescence (TADF) Molecules with Promising Electrically Pumped Lasing Property. *ACS Materials Lett.* **2022**, *4*, 487–496.
- (35) Yazdani, S. A.; Mikaeili, A.; Bencheikh, F.; Adachi, C. Impact of excitonic and photonic loss mechanisms on the threshold and slope efficiency of organic semiconductor lasers. *Jpn. J. Appl. Phys.* **2022**, *61*, 074003.
- (36) Abe, A.; Goushi, K.; Sandanayaka, A. S. D.; Komatsu, R.; Fujihara, T.; Mamada, M.; Adachi, C. Numerical Study of Triplet Dynamics in Organic Semiconductors Aimed for the Active Utilization of Triplets by TADF under Continuous-Wave Lasing. *J. Phys. Chem. Lett.* **2022**, *13*, 1323–1329.
- (37) Lindoy, L. P.; Mandal, A.; Reichman, D. R. Quantum dynamical effects of vibrational strong coupling in chemical reactivity. *Nat. Commun.* **2023**, *14*, 2733.